DOI: 10.21062/mft.2023.003 http://www.journalmt.com

Evaluation of Selected Technological Parameters for Selective Laser Melting of AlSi10Mg Metal Powder

Jozef Šutka (0000-0002-5205-5295), Denisa Medvecká (0000-0002-0553-885X)*, Radoslav Koňar (0000-0003-4588-2230), Marek Bruna (0000-0003-3742-7422), Marek Matejka(0000-0002-4156-5521)
Faculty of Mechanical Engineering, University of Zilina, Univerzitna 8215/1, 010 26 Žilina, Slovakia, E-mail: jozef.sutka@fstroj.uniza.sk, radoslav.konar@fstroj.uniza.sk, marek.bruna@fstroj.uniza.sk, marek.matejka@fstroj.uniza.sk, *Corresponding author: denisa.medvecka@fstroj.uniza.sk.

Reusing the powder across consecutive route cycles is typical in a Selective Laser Melting (SLM) process since it is more sustainable and cost-effective. The theoretical part of the paper is oriented on the explanationof the SLM method principle, construction, and parameters of the device Renishaw AM250 used for manufacturing samples made of AlSi10Mg aluminium alloy. The experimental part focuseson evaluating powders that had been used in the process for a long time with periodic 'rejuvenation'. The main aim will be to monitor whether the samples will be affected and if they achieved the required quality of mechanical properties and compare results with virgin powder and manufacturer sheets for virgin powders. The experimental part further describes the procedures and analysis of the microstructure of the samples. AlSi10Mg aluminium alloy was chosen because of an assumption that it will be sensitive to increased oxygen content. A strong affinity for oxygen uptake exists in AlSi10Mg. Therefore, preventing the contamination, careful handling is required.

Keywords: SLM, AlSi10Mg, powder, additive manufacturing

1 Introduction

Additive manufacturing (AM) has gained much attention in the manufacturing industry over the last 30 years, especially in modeling and prototyping. The ability to create a prototype in a short time from CAD models helps reduce production procedures. To meet the demands of the aerospace, automotive, and rapid tooling industries, the recent focus of AM research has shifted to the construction of complex metal components, including titanium-nickel alloys, which cannot be economically produced by using conventional technologies. Additive manufacturing's competitive position in the production of metal components is a function of theshape complexity of the products and the production volume. Fig. 1 shows that AM is suitable for the production of components with medium to high shape complexity in relatively small quantities. Compared to conventionaltechnologies, AM has several advantages. The first is the ability to complete automation from part design to pro- duction in a CAD / CAM environment, which reduces both production time and the amount of human intervention required for each new part. Although it is also possible to automate programming for CNC machining from CAD models, complex shapes require multiple clamping, which results in downtime and expensive calibration procedures. Another advantage of AM is its competitiveness in terms of production costs of components made of expensive materials such as titanium and nickel alloys in aviation. With AM, it is possible to produce one-component structures with a complex shape that would be difficult to manufature or could not be made by other technologies [1, 2].

1.1 SLM method

SLM has several advantages over traditional manufacturing methods, including fast production of finished products with sufficient density up to 99% without the need for expensive molds, high material utilization, direct production based on the CAD model, and a high degree of production flexibility. Furthermore, due to the additive and layered nature of production, the SLM process can produce a 3D part of any geometry that conventional production methods cannot achieve. The process consists of melting laser-applied layers of powder with a specific thickness range from 20 to 100 μm. The complete production usually takes 2-3 days for small parts and 5-8 days for large parts. The building material is a pure metal powder with a grain size of 20 μm. The components produced by this process have a high resolution and usually meet very small tolerances. The products have full density and mechanical properties equal to the mechanical properties of conventionally produced parts. These products can be modified by grinding, polishing, and other machining methods. The method is applied mainly in the aerospace and automotive industries and,

in the case of biocompatible materials, biomedicine. The advantage of this method stems from its flexibility, the possibility of using different metallic materials, and energy savings compared to conventional production methods [1-3].

1.2 Area of SLM application

In automotive (Fig. 1a), aerospace, and other industries - the precision and speed of component production allow industrial manufacturers to design, verify, and approve a product in a few days. The production technology enables the production of hybrid structures from biocompatible materials connecting the solid inner part with a porous surface treatment (Fig. 1b), which eliminates the need for further surface treatments and thus offers increased bioactivity. Since no tools are required, it is possible to produce different types, sizes, and shapes for each production task. Fashion, jewelry, and art (Fig. 1c) - the design involves the interweaving of different shapes and curves, which allows the titanium to be in a form that would not be possible to produce with conventional technology. Laser sintered parts are made into the final shape and polished to the desired appearance [3, 4, 5].

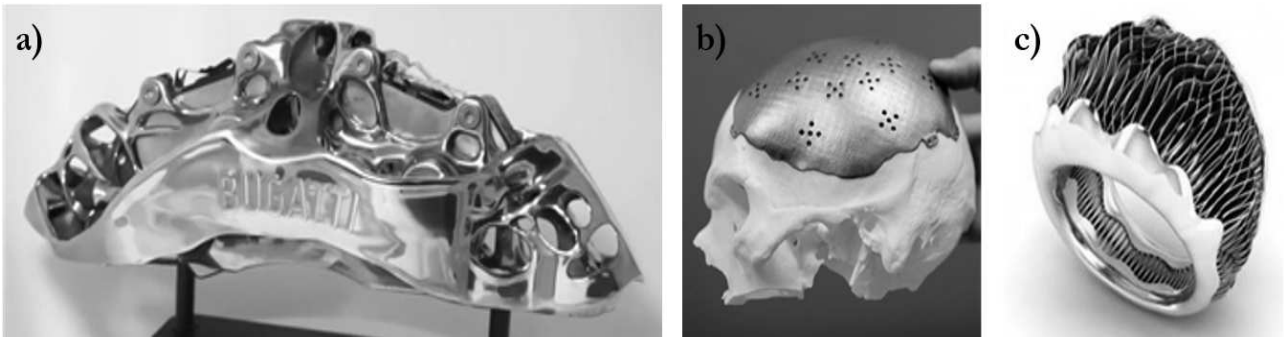

Fig. 1 *Areas of SLM application: (a) automotive industry; (b) biomedical engineering; (c) art (3DPRINTINGMEDIA. NETWORK 2016)*

2 Equipment, materials and methods

The equipment used for sample production is AM250 (Fig. 2) from the Renishaw company, the SLM techno- logy device. The AM250 allows air to be quickly extracted from the work area and immediately filled with pure argon gas to ensure a refined environment for reactive materials (titanium). AlSi10Mg is a typical casting alloy with suitable casting properties and is often used for thin-walled castings and complex shape products. It offers good strength, hardness, and dynamic properties, thanks to which it is also used for components exposed to heavy loads. AlSi10Mg components are ideal for applications where good thermal properties and low weight are required. The laser melting process is characterized by extremely fast melting and re-solidification. This results in mechanical properties with metallurgy characteristics in the post-production state (similar to T6 heat-treated castings). T6 heat treatment is not recommended for SLM components, but a heat treatment to remove stresses at 300 °C for 2 hours. Due to the layered nature of production, components have anisotropy that can be reduced or removed using appropriate heat treatment. AlSi10Mg is used in the aerospace and automotive industries due to its low weight [6-10].

Fig. 2 *AM250 device (Renishaw 2015)*

The experimental part evaluates the mechanical properties and structural characteristics of AlSi10Mg alloy powder produced by the SLM method without subsequent heat and surface treatment. Reused AlSi10Mg alloy in powder with a granulometry range from 20 to 30 μm was used as an experimental material to produce test samples. The chemical composition analysis of the used AlSi10Mg powder was performed on a Thermo Scientific QuantiX EDXRF device, and the resulting values are given in Tab. 1. Samples were modeled in Solidworks.

Tab. 1 *Chemical composition of AlSi10Mg [wt.%] AM250, 25 micron*

Si	Mg	Fe	Ti	Zn	Mn	Ni	Cu	Al
9.72	0.38	0.14	0.11	0.03	0.04	0.004	0.01	Bal.

Two sets of samples were made for experimental evaluation. The first set was made for a static tensile test (5 pcs) according to the ISO 6892-1 standard (disproportionate test bar with rectangular cross-section). The dimensions and orientation of tensile test samples are indicated in Fig. 3.

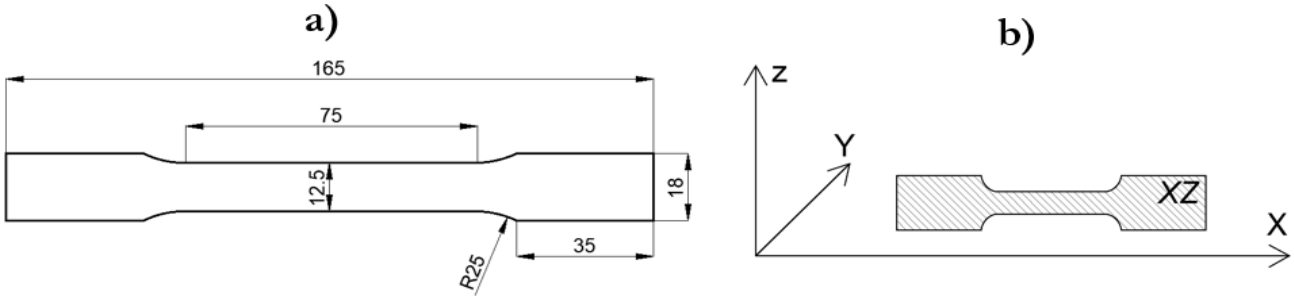

Fig. 3 *Static tensile test sample: (a) dimensions, (b) orientation*

The second set of samples was created to evaluate hardness using the CV-3000LDB Brinell hardness tester and observe the microstructure using optical microscope ZEISS LSM 700. Fig. 4 shows the direction of the manufacturing process. The wall thickness was 2 mm. The SLM technology was used for the production of both sets of samples using the Renishaw AM250 system (Renishaw plc, United Kingdom). The laserpower was set to 200 W, and the layer thickness was 25 μm. Support structures have been removed.

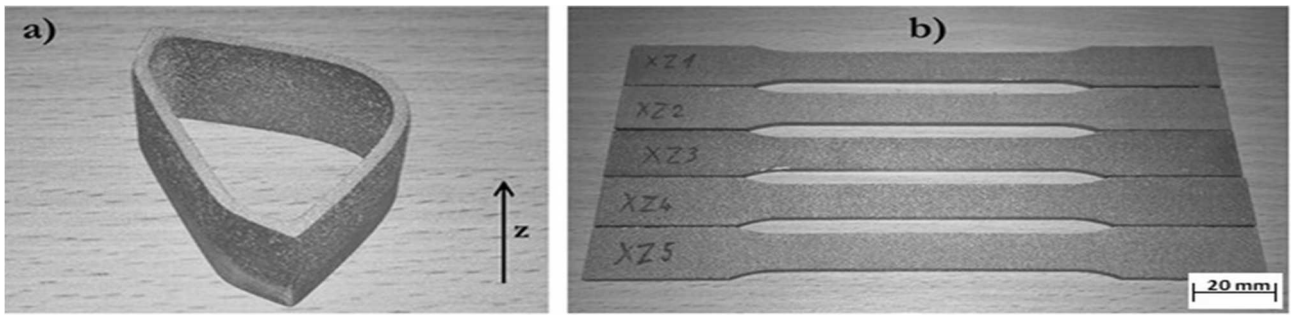

Fig. 4 *Experimental samples for: (a) hardness measurement and microstructure analysis, (b) static tensile test*

2.1 Microstructural analysis

The microstructure of the experimental samples of AlSi10Mg alloy is shown in Fig. 5, 6, and 7. The microstructure of the samples is given by the manufacturing process, and it refers to the individual laser transitions through layers. The porosity of the material and layering technique is shown in Fig. 5a) (Mosaic areas are visible). Individual layers and clusters of smaller pores are deposited in Fig. 5b) (layers parallel to the red arrow). The oxides in Fig. 5 are formed due to the usage of recycled (secondary) AlSi10Mg alloy powder. This is caused by oxidation of the protective powder's oxide coating Al_2O_3 as well as oxidation during production. Figure 6 shows the specific, very fine microstructure created by the SLM process, resulting from repeated rapid melting and subsequent material cooling. The cellular dendritic structure of the α-phase and the eutectic Si-phase network at the α-phase borders can be observed in the microstructures. The dimensions of these phases are much smaller than in casted products. The other two important aspects of this method are directional cooling and rapid solidification, which significantly influence the microstructure. The heat-affected area of nearby melting baths is represented by number 2 in Fig. 7a). In the melting bath itself (area 1), there is a fine cellular dendritic structure, and the same but larger structures are the results of thermal gradients in area 3 [11].

ISSN 1213–2489
e-ISSN 2787–9402

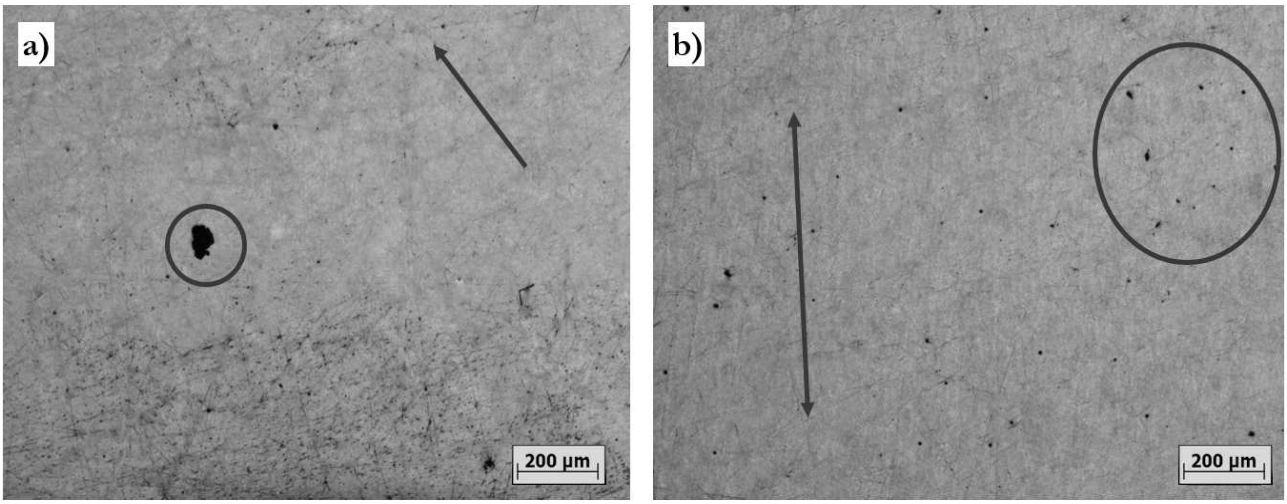

Fig. 5 *Texture of samples, mag. 50x. (a) in the XY plane, (b) in the XZ plane*

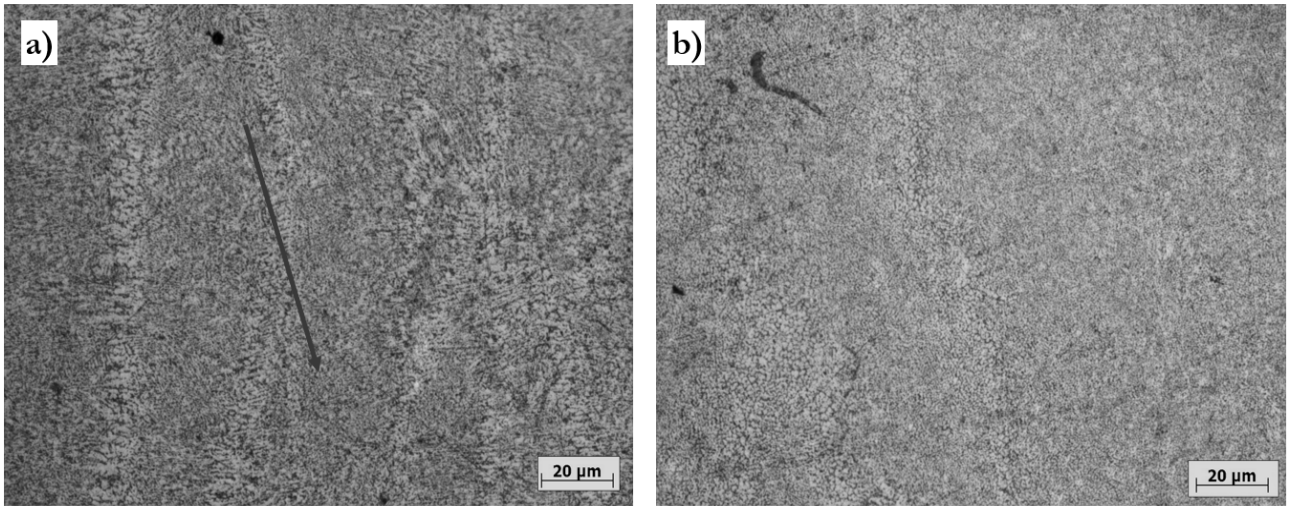

Fig. 6 *Texture of samples, mag. 500x. (a) in the XY plane, (b) in the XZ plane*

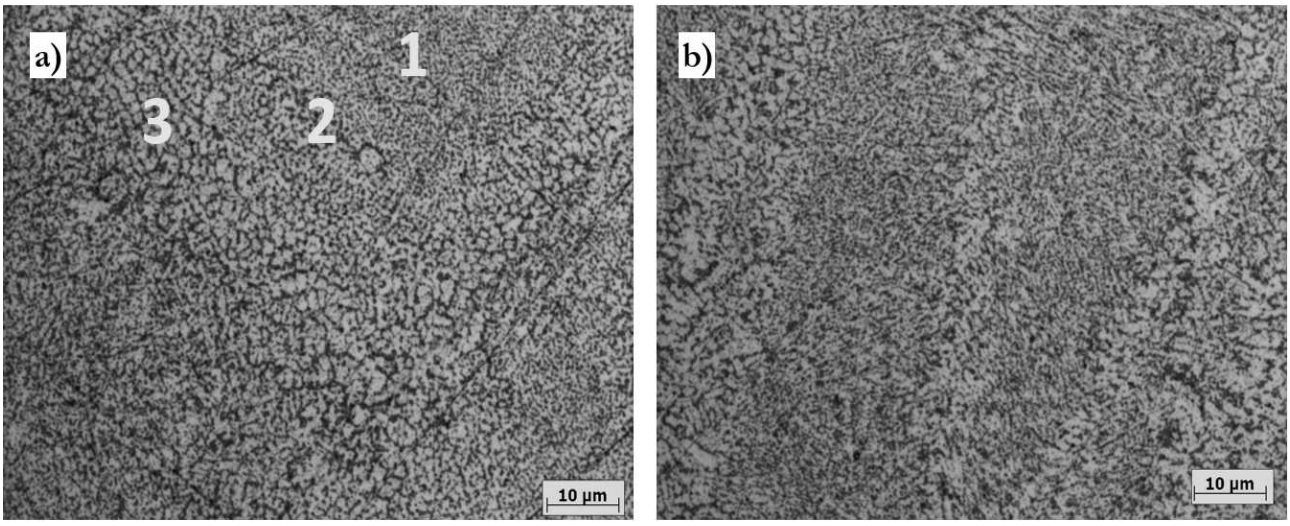

Fig. 7 *Texture of samples, mag. 1000x. (a) in the XY plane, (b) in the XZ plane*

2.2 Hardness evaluation

Brinell hardness measurement was performed on two specimens from the experimental sample in the formof untreated slabs with a thickness of 2 mm. One sample was produced by applying recycled powder (sample no. 1), and the second was by using virgin powder (sample no. 2). Each sample was subjected to eight measurements,with the arithmetic mean of the results calculated (Tab. 2).

Tab. 2 *Results of Brinell hardness measurements*

Measurement number	Sample no. 1 (HBW)	Sample no. 2 (HBW)
1	59	70
2	59	71
3	59	81
4	62	81
5	62	77
6	63	78
7	60	81
8	65	83
average	62	78

The final results showed lower values than those declared by the powder manufacturer. In comparison to the declared values (83 HBW), sample no. 1 reached 62 HBW and sample no. 2 78 HBW, what is a decrease of 25.3% for sample no. 1 and 6%. Low values for sample no. 1 are caused using a secondary powder. In the case of sample no. 2, results can be explained by the low wall thickness of the sample and measurements in the direction perpendicular to the construction direction of the sample.

2.3 Evaluation of the static tensile test

The static tensile test measurement was performed with the samples shown in Fig.8 and working diagrams were generated (example shown in Fig. 8). Sample XZ3 was produced by virgin powder, rest of the samples were produced by reused powder. Tensile strength and elongation results are shown in Tab. 3. Due to device failure, the max. deformation and elongation values for sample XZ1 could not be determined.

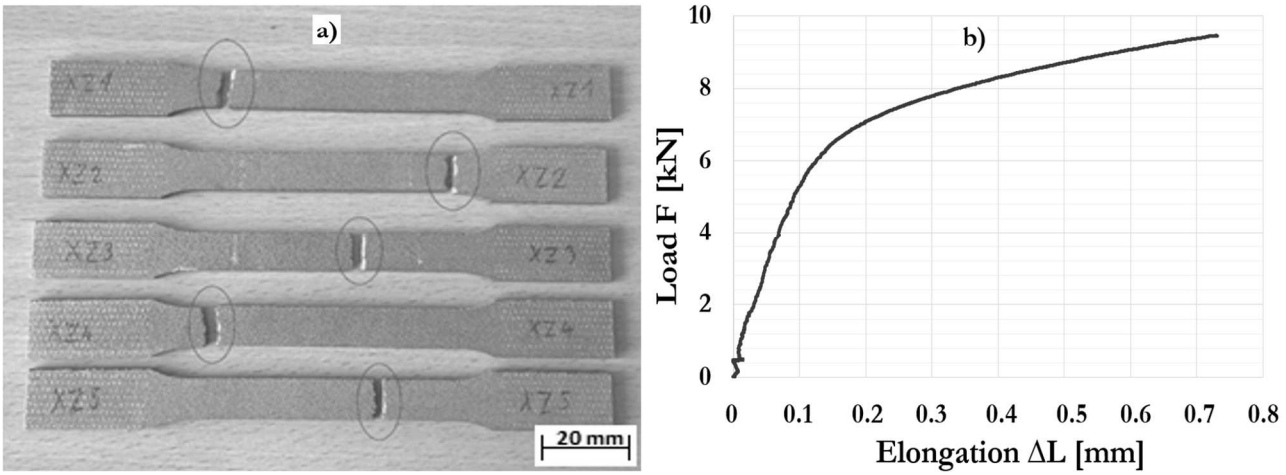

Fig. 8 *Static tensile test: (a) samples after tensile test; (b) example of a tensile load-elongation diagram of XZ2 sample*

Tab. 3 *Static tensile test results*

Sample	a_0 [mm]	b_0 [mm]	L_c [mm]	Max. Load [kN]	Tensile strength [MPa]	Max. Deformation [mm]	Elongation [%]
XZ1	12.6	3	50	10.3	273	-	-
XZ2				9.5	251	0.730	1.5
XZ3				11.5	344	1.086	2.6
XZ4				9.9	262	0.853	1.7
XZ5				8.4	222	0.456	0.9

The results of the static tensile test were lower than those declared by the supplier (Tab. 4). In Fig. 9 – 13, we can see the fracture surface of the samples after the static tensile test. Low strength and elongation values were caused by oxidation of the melting bath and pore formation. The highest value of strength and elongation was achieved by the sample XZ3 (Fig. 13) probably due to its location in the working chamber close to the inlet of the protective atmosphere. The mechanical properties of the XZ3 sample are most relative to the results declared by the supplier (Tab. 4). The XZ5 sample reached the lowest values due to the most significant amount of oxidation, which caused a high porosity on the fracture surfaces, which was directly involved in the formation of the fracture (Fig. 13).

Tab. 4 *Material properties declared by the manufacturer*

Indicator		Produced sample without surface treatment
Tensile strength [MPa]	Horizontal direction (XY)	400 ± 13
	Vertical direction (Z)	366 ± 30
Elongation [%]	Horizontal direction (XY)	4 ± 1
	Vertical direction (Z)	3 ± 1

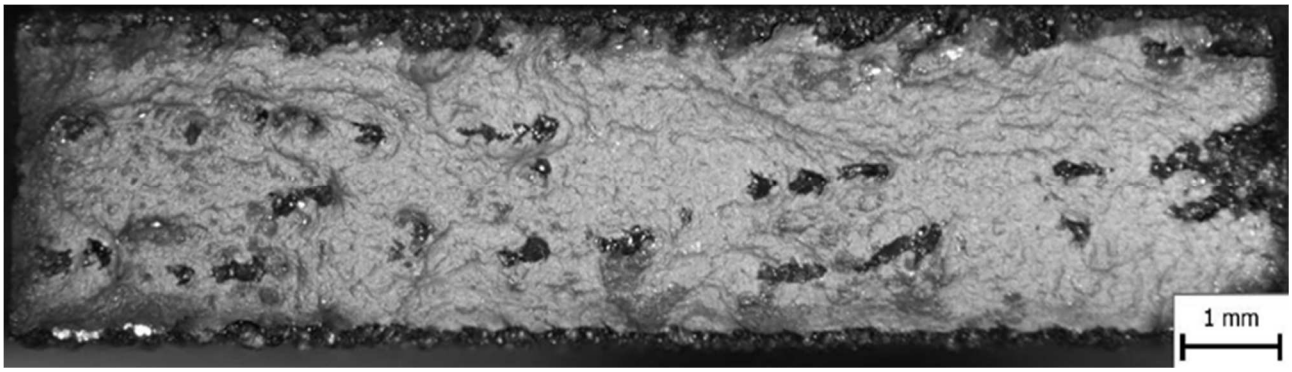

Fig. 9 *Sample XZ1*

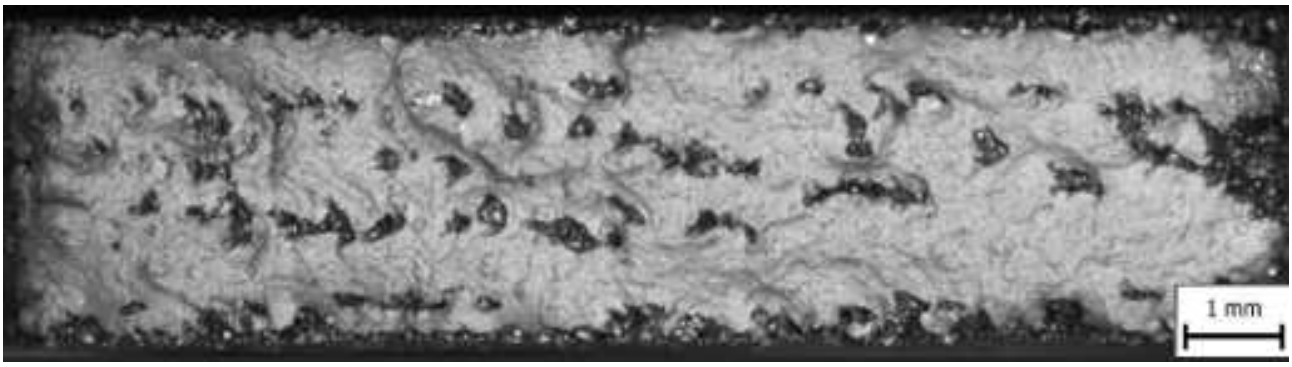

Fig. 10 *Sample XZ2*

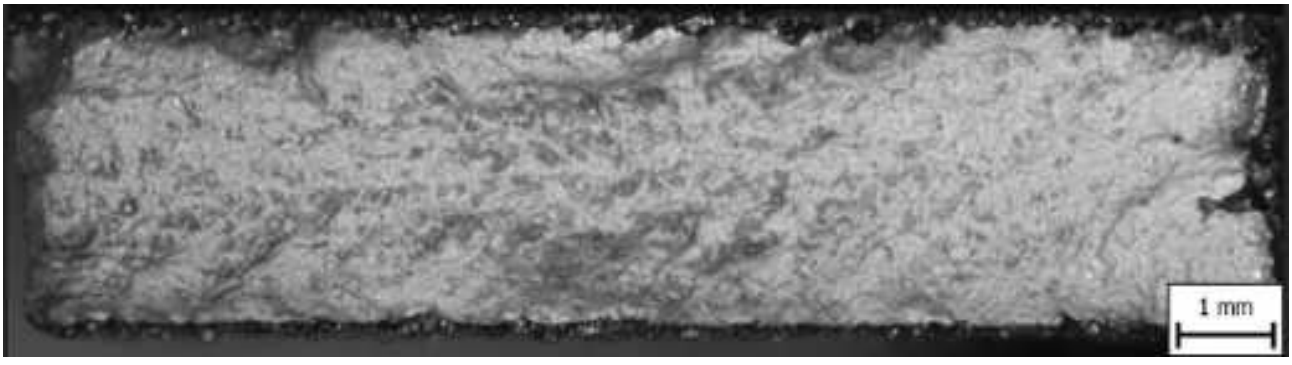

Fig. 11 *Sample XZ3*

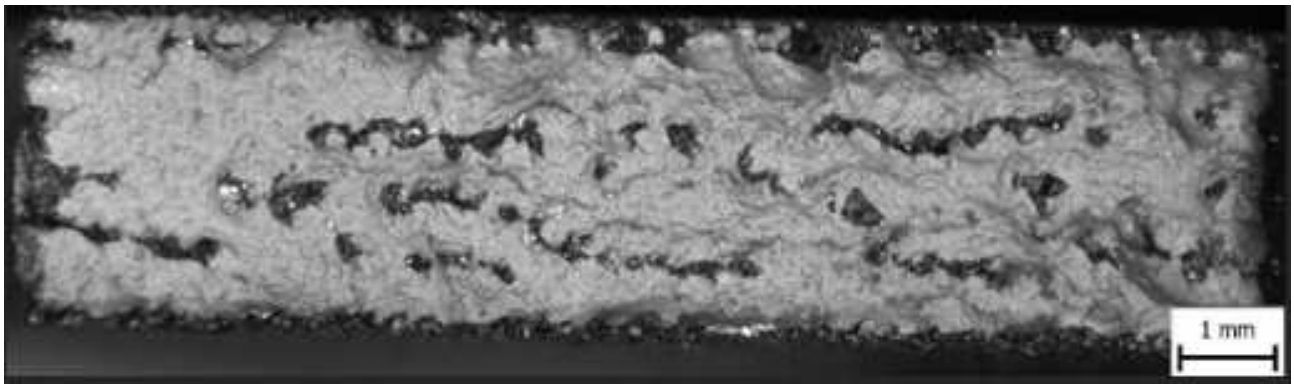

Fig. 12 *Sample XZ4*

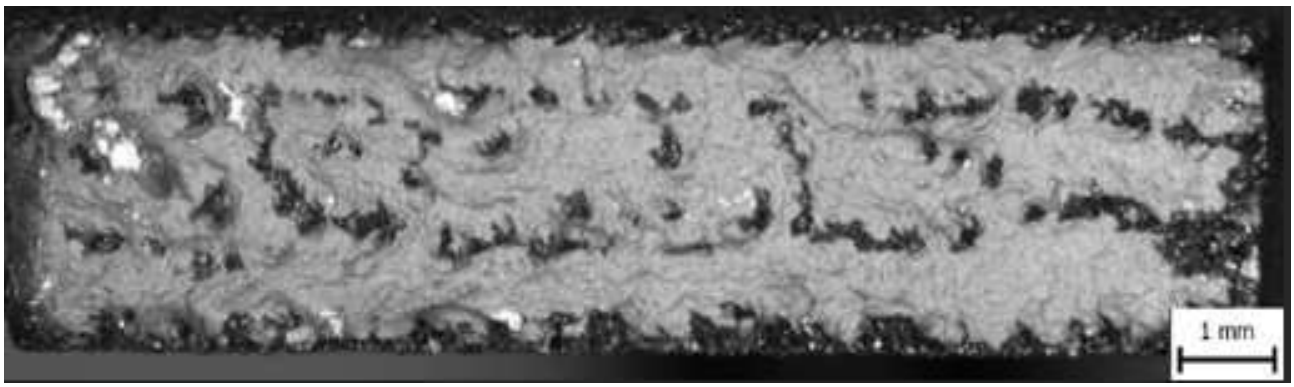

Fig. 13 *Sample XZ5*

3 Conclusions

The results of the experimental part led to the following conclusion:

- The microstructure of the samples prepared at the selected technological parameters is formed by the fine cellular dendritic structure of the α-phase and the network of eutectic Si-phase at the boundaries of the α- phase.
- The spreadability of recycled powder is better, as seen in the printing process. The bigger average particle size of recycled powder (due to the loss of fine particles during recycling) is coherent with this cohesiveness decrease.
- The tensile strength and elongation values were lower for the recycled powder, than stated in the material sheet due to the oxides coating of individual powder grains, which resulted in increased oxidation during the production of samples. The proof is also the high porosity on the fracture surfaces after the static tensile test.
- Future studies should focus on heat treatment (most products require post-treatment for final application) and the relationship between powder aging and other mechanical properties such as fatigue, including comparisons to the results reported in this paper.

Acknowledgments

This article was funded by the University of Žilina project 313011ASY4 „Strategic implementation of additive technologies to strengthen the intervention capacities of emergencies caused by the COVID -19 pandemic".

References

[1] SIMCHI, A. (2006). Direct laser sintering of metal powders: Mechanism, kinetics, and microstructural features. *Materials Science and Engineering a-Structural Materials Properties Microstructure and Pro- cessing*, 428(1- 2): pp. 148-158

[2] DING, D, et.al. (2015). Wire-feed additive manufacturing of metal components: technologies, develop- ments, and future interests. 2015. DOI 10.1007/s00170-015-7077-3.EIT *Biomedical engineering.* (2013). Aditívna výroba - Laserové sinterovanie kovov. Košice: s.n., 2013

[3] FATHOM. (2015). EOS // ALUMINIUM ALSI10MG. Studio Fathom. [Online] 2015. https://studiofa- thom.com/wp-

[4] 3D Systems. (2018). LaserForm® AlSi10Mg (A). *3D Systems*. [Online] 20. 3 2018. https://www.3dsy

[5] 3DPRINTINGMEDIA.NETWORK. (2016). Sisma Unveils myrev100 SLA 3D Printer. 2016

[6] KRIŠTOFOVÁ, P., ROUDNICKÁ, M., KUBÁSEK, J., PALOUŠEK, D., SUCHÝ, J., VOJTĚCH, D.(2019). Influence of Production Parameters on the Properties of 3D Printed Magnesium Alloy Mg-4Y-3RE-Zr (WE43). In: *Manufacturing Technology*, Vol. 19, No. 4, pp. 613-118. ISSN 1213-2489

[7] ROUDNICKA M., MISURAK M., VOJTECH, D. (2019). Differences in the Response of AdditivelyManufactured Titanium Alloy to Heat Treatment - Comparison between SLM and EBM[J]. *Manufacturing Technology*, 19(4):688-673

[8] OSAKADA K, SHIOMI M. (2006). Flexible manufacturing of metallic Products by selective laser meltingof Powder[J]. *International Journal of Machine Tools & Manufacture*, 2006, 46 (11): pp.1188-1193

[9] KURIC, I. et al., "Approach to Automated Visual Inspection of Objects Based on Artificial Intelligence," *Appl. Sci.*, vol. 12, no. 2, 2022, doi: 10.3390/app12020864

[10] HUNT, J.D., LU, S.Z. Numerical modeling of cellular/dendritic array growth: spacing and structure predic- tions. *Metall Mater Trans A 27*, 611-623 (1996). https://doi.org/10.1007/BF02648950